

Noise Stability of SIS Receivers

J.W. Kooi, G. Chattopadhyay, M. Thielman, and T.G. Phillips

California Institute of Technology, 320-47, Pasadena, CA 91125, USA.

R. Schieder

University of Koln, Dept. of Physics.

Abstract

There is a strong interest in the submillimeter astronomy community to increase the IF bandwidth of SIS receivers in order to better facilitate broad spectral linewidth and continuum observations of extragalactic sources. However, with an increase in receiver IF bandwidth there is a decrease in the mixer stability. This in turn effects the integration efficiency and quality of the measurement. In order to better understand the noise mechanisms responsible for reducing the receiver stability, we employed a technique first described by D.W. Allan and later elaborated upon by Schieder *et. al.* In this paper we address a variety of factors that degrade the noise stability of SIS receivers. The goal of this exercise is to make recommendations aimed at maximizing SIS receiver stability.

Keywords

“Allan” Variance, SIS mixer stability, low noise amplifier, gain stability, bias noise, temperature fluctuation noise, acoustic vibrations, Josephson noise.

I. INTRODUCTION

RA dio astronomy receivers in general look at very weak signals deeply embedded in noise. To extract the weak signals, synchronous detection (signal on - signal off) is typically employed. This is done by either slewing the whole telescope back and forth so as to get the beam on/off the source, or by moving the secondary mirror (subreflector) of the telescope at a certain rate. The problem in both these cases is the dead time between observations, i.e., chopping efficiency. A practical lower limit for slewing the whole telescope is typically 15 seconds, while chopping the secondary mirror can perhaps be as fast as 0.2 seconds (5 Hz). Frequency switching is possible and can be at a much higher rate, but suffers from a separate set of problems not discussed here.

If the noise in the receiver system is completely uncorrelated (white), it turns out that the rate of chopping (modulation frequency) has no effect on the final signal to noise ratio. This can be deduced from the well known radiometer equation (1) which states that the noise integrates down with the square root of integration time:

$$\sigma = \frac{\langle x(t) \rangle}{\sqrt{(B * \tau_{int})}} \quad (1)$$

Here σ is the standard deviation (rms voltage) of the signal, $\langle x(t) \rangle$ the signal mean, B the effective fluctuation bandwidth, and τ_{int} is the total integration time of the data set.

However, in practice the noise in radiometers, and in particular superconductor-insulator-superconductor (SIS) receivers, appears to be a combination of low frequency drift (correlated

noise), 1/f electronic noise and white (uncorrelated) noise. Hence, there is an optimum integration time, known as the ‘‘Allan’’ stability time (T_A), after which observing efficiency is lost. In actual synchronous detection measurements ‘‘n’’ samples of difference data (signal on - signal off) are taken, each with a period T . These differences are then averaged so that the total observed time equals $n * (2T)$. If the period T is larger than the ‘‘Allan’’ stability time (T_A) of the system, then apart from loss in integration efficiency, there will be a problem with proper baseline subtraction. This manifests itself in baseline ripples at the output of the spectrometer which severely limits how well the noise integrates down with time.

In this paper an effort has been made to understand the de-stabilizing effects on a radiometer output due to:

- LNA bias noise and gain fluctuations of the cryogenic low noise amplifier (LNA) immediately following the mixer.
- Temperature modulation of the SIS mixer and low noise amplifier.
- Acoustic noise pickup by the LNA and the local oscillator (LO).
- LO pumping of the SIS mixer.
- SIS mixer bias noise and the effectiveness of suppressing the Josephson effect [5] by means of a magnetic field applied across the SIS junction.

The goal of this paper is to focus attention to the output noise stability of radiometers and SIS receivers in particular. This work is especially pertinent in light of the present trend to construct very large IF bandwidth SIS and HEB receivers for spectroscopic and continuum observations of very weak extragalactic sources.

II. THEORETICAL CONSIDERATIONS

To optimize observation efficiency, it is important to find the best secondary mirror (sub-reflector) chopping rate. This requires a knowledge of the nature of the receiver noise fluctuations. In practice, we have employed a method developed by Allan [2], Barnes [3], and further elaborated on by Schieder *et al.* [4].

Following Schieder’s analyses of synchronous detection, two sets of contiguous data samples are taken, each with the same integration time (T). The first measurement is the signal $s(t)$, and the second measurement is the off-source reference signal $r(t)$. In the analysis, it is assumed that there is no dead time between the data samples. If we define the first measurement as:

$$S(T) = \int_0^T s(t) dt, \quad (2)$$

and the second measurement as:

$$R(T) = \int_T^{2T} r(t) dt, \quad (3)$$

then difference of the two measurements is

$$D(T) = S(T) - R(T). \quad (4)$$

Because we look at signals deeply embedded in the noise and are only interested in how the noise integrates down with time, we can make the simplification that there is essentially no signal present in $s(t)$. This means that on average $D(T) = 0$, and $s(t) = r(t)$. If μ is defined as the mean of $D(T)$ and σ^2 the variance of $D(T)$ then

$$\sigma^2(T) = \langle [D(T) - \mu]^2 \rangle = \langle D(T)^2 \rangle - \langle D(T) \rangle^2 \quad (5)$$

Here $\langle D(T)^2 \rangle$ is the mean (expectation value) of the difference squared and $\langle D(T) \rangle^2$ is the squared mean of the difference. But since $\langle D(T) \rangle$ equals zero we get

$$\sigma^2(T) = \langle [R_1(T) - R_2(T)]^2 \rangle . \quad (6)$$

From [2] we find that the ‘‘Allan’’ Variance is defined as:

$$\sigma_A^2(T) = 1/2 \sigma^2(T) \quad (7)$$

The mathematical treatment of the above expression can be found in [3] for different types of noise spectra. If the noise spectral density is represented by a power law, then

$$S(f) = f^{-\alpha}, \quad \alpha = [-1, 3] \quad (8)$$

and one finds that

$$\sigma_A^2(T) \propto T^{\alpha-1} \quad (9)$$

where $\alpha = 0$ stands for white (uncorrelated) noise, $\alpha = 1$ for ‘‘1/f’’ noise, and $\alpha \geq 2$ for correlated low frequency (drift) noise. Using a simple power law to characterize low frequency drift noise might not be correct. A more accurate representation would be to describe the noise by a correlation function, given by:

$$g(\tau) = \langle r(t) * r(t + \tau) \rangle . \quad (10)$$

The ‘‘Allan’’ variance can then be expressed as:

$$\sigma_A^2(T) = \frac{1}{T^2} \int_{-T}^T (T - |\tau|)(g(\tau) - g(T + \tau)) d\tau. \quad (11)$$

Because we are interested only in integration times less than the correlated (drift) noise time scale, the correlation function can be expanded in a power series with only a few terms:

$$g(\tau) = g(0) - a\tau^\beta \pm \dots, \quad \beta = 1, 2, \dots \quad (12)$$

From equation (11) we get

$$\sigma_A^2(T) \propto T^\beta. \quad (13)$$

Combining equation (9) and equation (13) we find that for a noise spectrum that contains drift, white noise, and 1/f noise that the ‘‘Allan’’ variance takes the form:

$$\sigma_A^2(T) = aT^\beta + \frac{b}{T} + c, \quad (14)$$

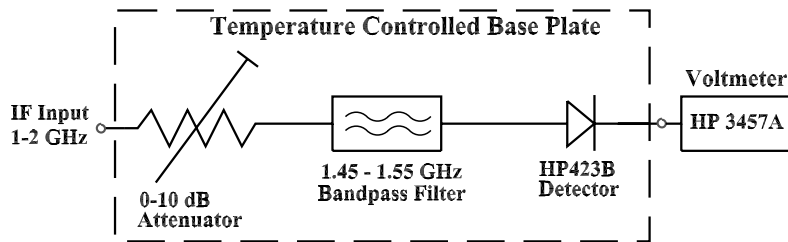


Fig. 1. Configuration of the “Allan” variance measurement setup. Unless otherwise stated, we have used a 50 mS sample time and 100 MHz bandwidth filter to acquire the data.

where a , b , and c are appropriate constants. For short integration times, the variance decreases as $\frac{1}{T}$, as expected from the radiometer equation (1). For longer integration times, the drift will dominate as shown by the term aT^β . In that case, the variance starts to increase with a slope β which is experimentally found to be between 1 and 2. On certain occasions, it is observed that the variance plateaus at some constant level. This is attributed to the constant factor and is representative of flicker or $1/f$ noise in the electronics.

Plotting $\sigma_A^2(T)$ on a log-log plot demonstrates the usefulness of this approach in analyzing the radiometer noise statistics. For reference, a slope of $(\frac{1}{T})$ has been drawn in all figures. This represents the uncorrelated (white) noise part of the spectrum. The minima in the plot gives the “Allan” time (T_A), the crossover from white noise to $1/f$ or drift noise. For the sake of optimum integration efficiency, one is advised to keep the integration time well below the system’s “Allan” time.

Finally, it is often of interest to estimate what happens to the “Allan” stability time if the IF bandwidth of the radiometer is increased. Solving equation (14) for T as a function of receiver IF bandwidth we get:

$$T_A \propto B_{IF}^{-\left(\frac{1}{\beta + 1}\right)}, \quad \beta = 1 - 2. \quad (15)$$

B_{IF} presents the IF bandwidth and β the slope of the drift noise as discussed above. As the uncorrelated (white) noise component of the mixer spectral output power is reduced, the intersect between radiometric (1) and drift noise (13) equations occurs at an earlier time. Where exactly the two curves intersect depends on the statistical nature of the long term drift. It should be noted that all data presented in this paper have been taken with a 100 MHz bandpass filter.

III. MEASUREMENT SETUP AND CALIBRATION

The measurement configuration is shown in Fig. 1 and consists of a variable 0-10 dB step attenuator, a 100 MHz bandwidth filter, centered at 1.5 GHz, and a Schottky power detector. RF signal power on the detector has been kept constant to within 1 dB throughout the measurements. The whole unit is bolted to a 1 cm thick aluminum base plate and is thermally insulated from the surroundings. The output of the crystal diode is connected to a GPIB controlled 8.5 digit HP voltmeter. To test the stability of the system we ran a series of calibration tests such as the one shown in Fig. 2. The voltmeter is stable to at least 10

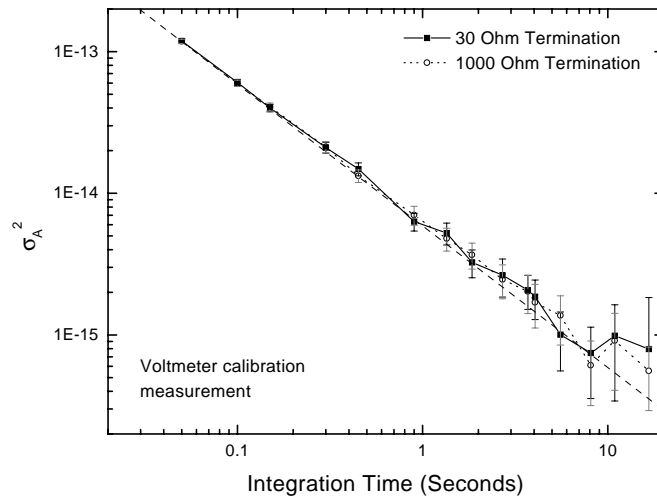


Fig. 2. HP 3457A Digital Voltmeter noise stability performance. The input to the voltmeter was terminated into 30 and 1000 Ohms. The two curves were taken several days apart, which indicates the stability of the measurement setup and HP voltmeter. The dashed line has a slope of $1/T$.

seconds, which turns out to be adequate for continuum noise stability measurements of SIS receivers with IF passbands ≥ 100 MHz. All data presented in this paper is a statistical average of six 5 minute data runs, consecutive in time.

IV. IF TOTAL POWER BOX STABILITY MEASUREMENTS

An IF total power box consists of a series of commercially purchased amplifiers, filters and couplers. The passband in use at the Caltech Submillimeter Observatory (CSO) is 1-2 GHz, and has an overall gain of 40-50 dB. With such a large gain, extreme precautions need to be taken to insure stable operation. The individual amplifiers are mounted on isolated pedestals which are heated to $\approx 45^\circ\text{C}$. AC power is separated from the RF signal by different compartments inside the chassis. The chassis is built from thick aluminum stock, which provides for a long thermal time constant.

In Fig. 3 we show the measured IF power box stability in the laboratory and at the CSO. The inputs to the total power box were terminated with a $50\ \Omega$ load. The IF power box at the CSO has a slightly shorter “Allan” variance time (≈ 7 seconds) than a similar IF power box in the laboratory (≈ 10 seconds). The difference is attributed to the much higher RFI and EMI noise environment at the observatory.

V. LOW NOISE AMPLIFIER (LNA) GAIN FLUCTUATIONS

Recently Schieder *et. al* have studied gain fluctuations of a 4-6 GHz cryogenic GaAs amplifier at both room and liquid helium (4.2K) temperatures with a Köln built Acousto Optical Spectrometer (AOS) [11]. The particular amplifier under discussion was built for the Submillimeter Array (SMA) project by the National Radio Astronomy Observatory [6].

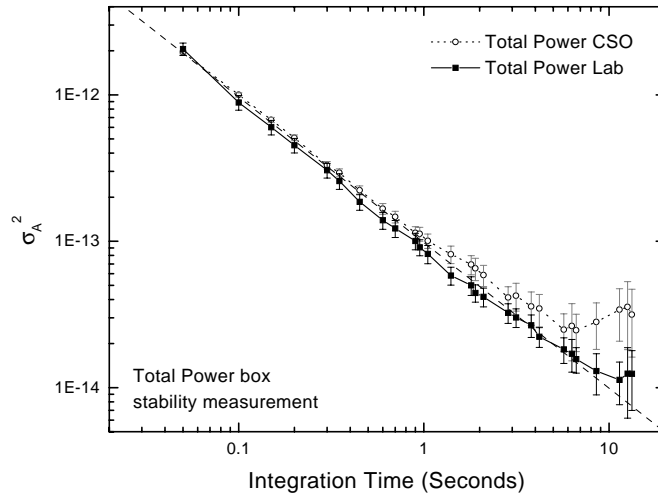


Fig. 3. IF Total Power box stability measurements in a 100 MHz bandwidth window at the Caltech Submillimeter Observatory (CSO) and in the laboratory. Note that the ambient EMI/RFI noise environment at the CSO is much higher than in the laboratory.

The amplifier gain fluctuation, as measured differentially by subtracting two distinct AOS channels and integrating with time, was shown to be completely negligible when compared to the observed SIS receiver output noise fluctuation.

Schieder's measurements were performed with the amplifier mounted on the liquid helium stage of the cryostat. This however is different from the situation at many observatories. Frequently closed cycle helium expansion refrigerators are used in cryostats to reduce or eliminate the use of liquid helium. The refrigeration action vibrates the dewar, and may in fact produce small scale temperature fluctuations on the cryostat's temperature stages (usually 80K and 15K). Since the low noise amplifier (and sometimes even the mixer) is mounted to an active cooled stage, it is highly probable that acoustic vibrations and thermal fluctuations modulate the LNA and mixer, hence compromising the stability of the receiver.

To better understand the process, or mechanism, by which drift noise is introduced in the receiver a series of experiments were performed. These experiments use a 1-2 GHz balanced amplifier based on a design by Padin *et. al* [7] but adapted by the authors to suit the needs of the CSO. This design uses GaAs Pseudomorphic HEMT devices very similar to those used in the NRAO 4-6 GHz amplifier in Schieder's experiment. For this reason it was felt not necessary to repeat Schieder's gain fluctuation measurements.

VI. LNA BIAS NOISE AND ACOUSTIC PICKUP

We first mounted an amplifier with terminated input on the liquid helium stage of a passive cooled IR-Labs dewar [8] and compared the result against the same amplifier mounted on the liquid helium stage of an active cooled hybrid style cryostat [9][10]. The results are shown in Fig. 4. There appears to be little difference between the two dewars. Note that the $(\frac{1}{T})$ slope

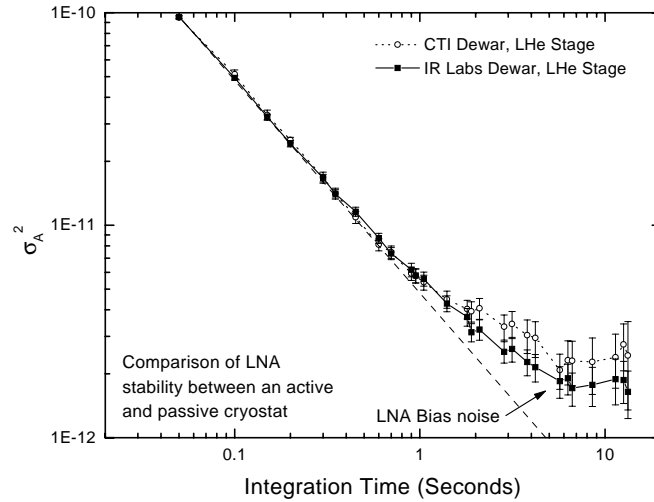


Fig. 4. Stability measurement of a low noise amplifier in an CTI cooled hybrid style dewar and a passive liquid helium cooled dewar. In both cases the amplifier is mounted directly to the 4.2 K liquid helium stage. The deviation from the $1/T$ slope (dashed line) is most likely due to low frequency noise on the amplifier bias line.

begins to deviate from the 100 % uncorrelated noise slope (equation 14) at about 1 second of integration time. The IF total power box stability measurement in the laboratory, shown in Fig. 3, does not deviate from the $(\frac{1}{T})$ slope until approximately 10 seconds however! The deviation from the $(\frac{1}{T})$ slope in Fig. 4 shows a loss of integration efficiency and is significant in that it indicates the presence of low frequency noise on the LNA bias line. This noise modulates the gate of the GaAs HEMT slightly thereby degrading the amplifier's long term noise stability. A resistive voltage divider network on the gate may provide the needed noise immunity. Note that the "Allan" time has only degraded slightly, from 10 to 8 seconds, as a result of the bias noise.

In the next experiment we transferred the balanced amplifier to the active cooled 15K stage of the hybrid cryostat, everything else being the same. The amplifier low frequency baseband spectrum was observed by connecting a spectrum analyzer to the output of the crystal detector in Fig. 1. The baseband spectrum reveals the fundamental 1.2 Hz compressor action along with many harmonics (Fig. 5).

To find out whether harmonics are introduced acoustically or thermally, we remounted the amplifier on the liquid helium stage, but this time on four 1 cm long Teflon standoffs. This had the effect of vibration isolating the amplifier from the active cooled 15 K stage. The amplifier was then heat strapped to the 15 K stage with a 12 mm wide, 5 cm long, 2 mm thick copper strip. As can be seen in Fig. 6 the response of the vibration isolated amplifier deviates rather quickly from the $(\frac{1}{T})$ slope ($T_{int} = 0.1$ Seconds). Presumably this is due to the not too ridged mount in our experiment, or perhaps a too solid connection (small mechanical time constant) to the active cooled stage. The overall improvement in integration

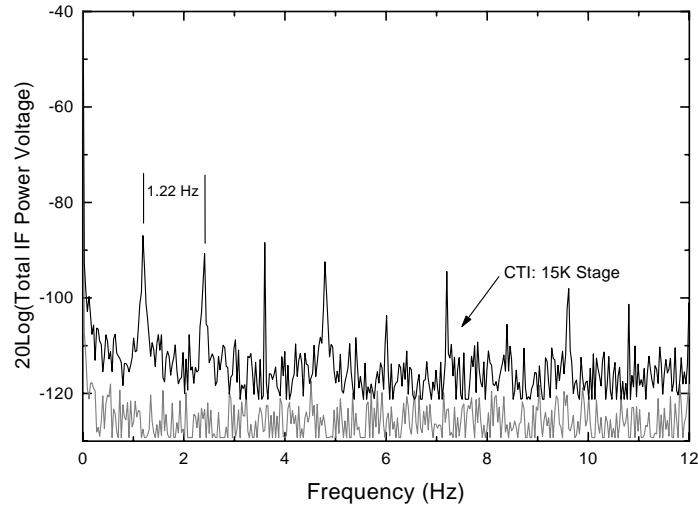


Fig. 5. Baseband spectrum of a low noise amplifier mounted on an active cooled (15K) stage and liquid helium (4.2K) stage. The two plots are offset to better show the difference.

time is seen to go from 0.8 seconds to 7 seconds if some loss in integration time efficiency is tolerated. This result can be improved upon with a more rigorous design however. The

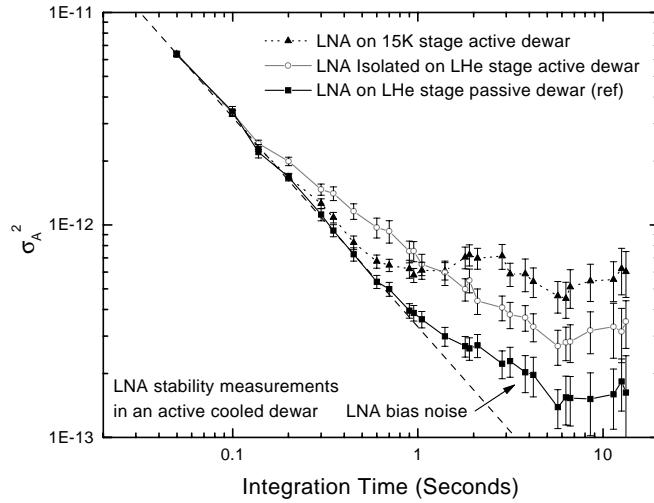


Fig. 6. LNA stability measurements with the amplifier mounted to the active cooled (15K) stage and to the liquid helium (4.2K) stage. In the latter case the amplifier was vibration isolated by mechanically connecting it to the LHe stage but thermally strapping it to the 15K active stage. The response in the case of a passive dewar has been included as a reference.

measured baseband spectrum in this case is shown as the bottom trace in figure 5. It is unclear what components in the amplifier, or wiring, are sensitive to mechanical vibrations. Presumably the result presented here will vary with different style amplifiers and mounting configurations. Nevertheless, it appears good practice that the LNA be vibration isolated by mounting it to the liquid helium stage, while at the same time be thermally connected to an actively cooled stage in the dewar to conserve helium. It is expected that at higher IF frequencies acoustic pickup will become less of an issue because amplifiers are more planar in design.

VII. LNA AND SIS MIXER TEMPERATURE FLUCTUATIONS

Another means by which a radiometer's stability can be compromised is when the mixer and IF amplifier (LNA) are subjected to temperature fluctuations. A slow change in the physical temperature of the mixer, or amplifier, results in a change in receiver gain. Hence, temperature fluctuations manifest themselves as low frequency drift noise at the output of the receiver.

Because most, if not all, sensitive receivers utilize some kind of active cooling system, it is of interest to quantify the maximum allowed temperature drift given a certain "Allan" stability time. We assume an IF output signal of the form:

$$s(t) = s_o(1 + g_t t). \quad (16)$$

Here g_t is defined as the normalized drift in system gain, and s_o the nominal total power at $t=0$. Defining m_t as the slope of the IF output drift with respect to time, it can be seen that $g_t = m_t/s_o$.

If we take two contiguous measurements, like the ones described by equation (2) and equation (3), and define

$$Z(T) = [S(T) - R(T)]/R(T), \quad (17)$$

we obtain the variance of the relative drift:

$$\sigma^2(drift) = \langle [Z(T) - \mu]^2 \rangle = \langle Z(T)^2 \rangle - \langle Z(T) \rangle^2. \quad (18)$$

Since the mean of $Z(T) = 0$ (Section II), equation (18) simplifies to:

$$\sigma^2(drift) = \langle [(S(T) - R(T))/R(T)]^2 \rangle = (g_t * T)^2. \quad (19)$$

This corresponds to a $\beta = +2$ slope for the drift contribution in the "Allan" plot (equation (14)). At the same time we have for the radiometric noise (1)

$$\sigma^2(rf) = \langle [(S(T) - R(T))/R(T)]^2 \rangle = \frac{2}{B * T}, \quad (20)$$

where B is the bandwidth and T is the integration time of the data sample.

From equation (7) and using the constant c to represent the 1/f electronic noise we have:

$$\sigma_A^2(T) = (g_t * T)^2 + \frac{2}{B * T} + c. \quad (21)$$

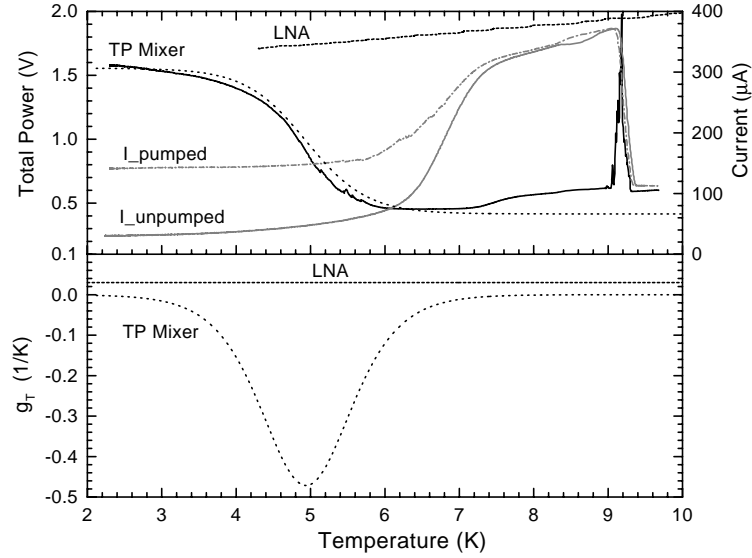


Fig. 7. SIS mixer and LNA gain sensitivity as a function of temperature. Note the large difference in sensitivity to temperature between the LNA and LO pumped SIS mixer. The pumped and unpumped SIS current has been included for reference. In the experiment the SIS junction was constant voltage biased at 2.2 mV, the peak of the total power response at 4.2 Kelvin. The computed normalized slope $g_T = (1/s_o * dP/dT)$ is shown in the bottom half of the figure and used in equation (25). Above 9.2 Kelvin the niobium film ceases to be a superconductor and the LO pumped junction current drops sharply.

Differentiating with respect to T gives the “Allan” stability time minima:

$$T_A = (g_t^2 B)^{-\frac{1}{3}} . \quad (22)$$

Equation (22) can now be re-written so that given a desired “Allan” time we obtain an estimate for the maximum allowed rate of change in system gain:

$$g_t = (T_A^3 * B)^{-\frac{1}{2}} . \quad (23)$$

For example, if a radiometer requires a broadband total power continuum detection of 4 GHz and has a required “Allan” stability time of 1 second, we find a maximum allowed drift in system gain of $1.4 * 10^{-3}$ % per second (5.7% per hour).

Having calculated the allowed drift in gain, we can now get an idea of the maximum temperature fluctuation a SIS mixer and low noise cryogenic GaAs HEMT amplifier may be subjected to. Re-writing equation (16) in terms of temperature dependence gives:

$$s(t) = s_o(1 + g_T(T - T_o)) , \quad (24)$$

where g_T is defined as the normalized temperature dependent drift of the system. Let m_T be the slope (dP/dT), a property of the SIS mixer and amplifier, then $g_T = m_T/s_o$.

To obtain g_T for the 1-2 GHz balanced amplifier and LO pumped double slot SIS mixer [12], we performed the following experiments. First, the LNA was gradually heated from

4.2 Kelvin to 10 Kelvin in a time span of 1 hour (LNA input load at 4.2 Kelvin), while continuously recording the IF total power and amplifier physical temperature. In the second experiment we pumped a SIS mixer with LO power [12] and over the course of an hour varied its temperature from 2.16 Kelvin to 9.6 Kelvin. The temperatures referred to in the text were measured at the outside of the mixer and amplifier block. During the LO pumped mixer experiment the LNA remained unheated at 2.16 Kelvin. g_T for both the mixer and low noise amplifier can be obtained directly from Fig. 7b. The SIS mixer has a negative temperature dependence, while the low noise amplifier has a positive and constant temperature dependence.

As the physical temperature of the mixer in figure 7 is changed from 2.16K to 6K we see the mixer output noise drop in an exponential manner. The dotted line in Fig. 7a is a best fit Fermi function. As the temperature of the mixer block is increased from 2.16K to 6K only a minimal change in the junction's unpumped current (shot noise) is observed. The change in total power is to a very large extent caused by the temperature dependent conversion gain of the mixer. Above 7.2K we observe a jump in total power, which is attributed to the by now large leakage current (shot noise) in the junction. At 9.2 Kelvin the niobium film ceases to be a superconductor and the LO pumped junction current drops sharply. Note, that the SIS mixer conversion gain sensitivity to temperature peaks around 4.9 Kelvin. This is unfortunately close to the 4.2 Kelvin bath temperature SIS mixers usually operate at (1 Bar atmospheric pressure). Moving to an high altitude site (600 mBar) improves the mixer conversion gain by $\approx 7-8\%$ [14] and reduces the mixer's sensitivity to temperature fluctuations. Reducing the helium bath temperature to 1.5K would reduce this to a minimum.

Combining equations (16) and (24) we obtain the maximum allowed temperature change:

$$\delta T = t * \frac{g_t}{g_T} \quad (25)$$

g_t is obtained from equation (23) and g_T can be obtained from figure 7b.

In the example of the 4 GHz bandwidth total power continuum detection (worst case scenario) we estimate a maximum allowed gain drift of $14 * 10^{-4} \%$ per second given a 1 second "Allan" time. At 4.2 Kelvin this gain drift equates to an allowed temperature drift of 470 $\mu\text{K}/\text{second}$ for the LNA and 66 $\mu\text{K}/\text{second}$ for the LO pumped SIS mixer! In high resolution spectrometer mode with a channel bandwidth of 100 KHz, 1 second of "Allan" stability time and an high altitude Helium bath temperature of 3.6 Kelvin, we find a maximum temperature fluctuation of 106 mK/second for the LNA and 48 mK/second for the SIS mixer (13.8 mK/second at 4.2 Kelvin bath temperature).

VIII. RECEIVER STABILITY WITH AN SIS JUNCTION BIASED ABOVE THE ENERGY GAP

In addition to acoustic, bias, and thermal noise pickup by the low noise amplifier, there is also a chance that the SIS receiver stability is compromised by low level noise on the mixer bias line. When we bias a SIS junction in the resistive region above the superconducting energy gap (for niobium $\frac{2\Delta}{e} = 2.8 \text{ mV}$) we eliminate gain variation effects, since the mixer has zero gain.

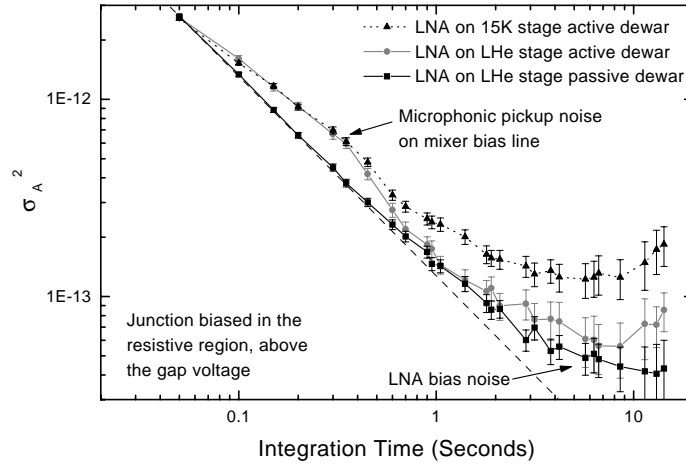


Fig. 8. Dual polarized cross-slot SIS mixer biased above the gap (5 mV). Mixer and low noise amplifier were mounted in a liquid helium (passive) dewar, and CTI cooled hybrid (active) dewar. In the hybrid dewar, the LNA was mounted two ways; directly onto the 15K active cooled stage and to the LHe stage.

Thus by comparing “Allan” variance stability plots of the LNA (Fig. 4) with “Allan” variance plots of the SIS mixer biased above the gap (Fig. 8) we study the effect of mixer bias fluctuation noise. The laboratory measurements described in this paper were taken with a 550 GHz dual-polarization SIS mixer [12]. The experiments described were taken under the following conditions:

- LNA mounted in a passive, IR-Lab, liquid helium dewar (ideal).
- LNA mounted to the LHe stage of an active cooled hybrid dewar.
- LNA mounted to the 15K stage of an active cooled hybrid dewar.

In the passive cooled dewar, we observe that the mixer output noise integrates down for roughly 10 seconds (bottom curve, Fig. 8). The manner in which the noise integrates down turns out to be nearly identical (within the error-bars) to the LNA noise, as shown in Fig. 4. The deviation from the $\frac{1}{T}$ slope at 1 second in Fig. 8 is clearly due to the LNA and not the SIS mixer. This experiment shows that the mixer is less susceptible to bias noise than the LNA. Presumably this is because of the much larger gain (30 dB vs -3dB in the case of the mixer) of the low noise amplifier.

The center curve in Fig. 8 shows both LNA and SIS mixer mounted to the LHe stage of the active hybrid style dewar. The top curve is for the case when the LNA is moved onto the active cooled 15K stage. In both these situations we see a consistent bump at 0.3 seconds. This effect has not been seen in measurements of the LNA alone, and is attributed to acoustic (CTI compressor harmonic) noise pickup on the mixer bias line inside the active cryostat. To verify this theory Schieder *et. al* ran simulations with Lorentzian shaped pulses

on top of a white noise power spectrum. The amplitude of these pulses was only 0.15 % of the mean data, practically invisible in the primary data set. His computer simulations indicate that the location and the shape of the bump does not depend very much on the repetition frequency but on the details of the structure of the pulses. Using these simulations we are able to closely match the experimental data and confirm that the bump is indeed due to acoustic pickup induced by the refrigeration action of the hybrid dewar.

The SIS mixer bias circuit used in the experiments consists of a resistive bias network with ~ 35 dB of noise isolation. Even so we see the effect of microphonic noise, which is consistent with Schieder’s impulse response simulations. Note that the “Allan” variance stability time for a SIS-mixer/LNA combination mounted to the LHe stage of the passive dewar and active cooled hybrid dewar is practically the same (bottom and middle curve, Fig. 8). This demonstrates that the interference noise does integrate down with time, though not as efficiently as one may like. In both these cases we measure an “Allan” time of roughly 8-9 seconds. This demonstrates that stable receiver operation with an active cooled cryostat is possible, with proper care and precautions.

As discussed, in the third experiment we moved the LNA (active cooled dewar) from the LHe stage to the active cooled 15K stage, keeping everything else the same. It is instructive to observe the drastic reduction in integration efficiency and “Allan” variance time (top curve, Fig. 8) due to acoustic vibrations of the low noise amplifier.

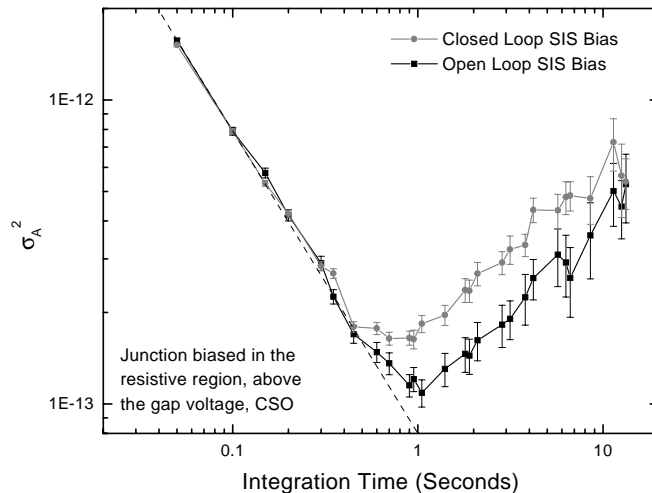


Fig. 9. 345 GHz receiver stability with the mixer biased at 5mV. No LO power was applied. “Allan” stability times are 1 and 2 seconds respectively for the open and closed voltage feedback bias configurations. The LNA is mounted on a 15K actively cooled stage. Data was taken at the Caltech Submillimeter Observatory.

IX. RECEIVER STABILITY WITH THE SIS MIXER BIASED IN OPEN AND CLOSED FEEDBACK LOOP MODE

We have studied the receiver stability with the SIS junction biased above the gap in both “open” and “closed” loop voltage bias modes. Open loop is without bias feedback, while closed loop uses feedback to keep the voltage on the junction fixed. In the laboratory measurements discussed in section VIII we did not observe a difference between open and closed feedback bias methods. This is in contrast to the data taken at the CSO with a 345 GHz waveguide receiver [13], shown in Fig. 9. At the CSO the “Allan” variance time is a factor of two better without the voltage feedback than with the voltage feedback bias. We believe that this is due to the much higher ambient noise background at the observatory compared to the laboratory environment. The observatory is essentially a near perfect Faraday cage, with all the noise generated on the inside. The reference signal for the closed loop voltage is derived inside a SIS bias box, external to the dewar. Although the feedback loop bandwidth is only 80 Hz and the SIS bias circuit provides more than 40 dB of isolation, EMI noise is evidently still present on the SIS junction. It is expected that reducing the loop bandwidth will filter some of the noise, though not all. As a precaution, it may therefore be advisable to have a SIS junction bias source with two loop bandwidth’s. One for tuning the mixer (fast time constant) and the other for observation mode (slow time constant). It should be noted that the receiver used in Fig. 9 has the amplifier mounted directly on a 15K actively cooled stage. We are currently investigating means of isolating the LNA from vibrations.

X. RECEIVER STABILITY WITH A 460 GHz LO PUMPED SIS JUNCTION

In Fig. 10 we show the effect of acoustic vibrations on a local oscillator (LO) pumped SIS mixer [12]. In all of the experiments, great care has been taken to null out the Josephson oscillations in the junction [5]. The measurements were taken under the same conditions as in Section VIII.

Under the ideal condition of a passive cooled cryostat, we see that the noise integrates down nearly perfectly to 6 seconds. When we compare this result with the 9-10 second unpumped “Allan” variance time from the measurements with the junction biased above the gap voltage (Fig. 8), it is suggestive that Josephson noise in the superconducting junction, or bias noise induced gain variation, is limiting the receiver stability time. Note also that the slight deviation (bottom curve, Fig. 10) from the $\frac{1}{T}$ slope is once again due to the LNA bias noise (see Fig. 4). We used a free running Gunn oscillator followed by a quadrupler to pump the mixer. The whole assembly was mechanically disconnected from the passive cooled dewar. Ample time was given for the local oscillator unit to reach thermal equilibrium. The LO was injected quasi-optically by means of a 12 μm beamsplitter mounted to the side of the dewar.

Next, we changed from the passive dewar to the active cooled hybrid cryostat [9]. The LNA was mounted to the liquid helium stage of the hybrid dewar. The 460 GHz local oscillator chain and LO injection beamsplitter were physically attached to the side of the dewar, and were thereby subjected to the mechanical vibrations of the dewar. The result is shown in Fig. 10, center curve. Not only has the “Allan” variance time of the receiver

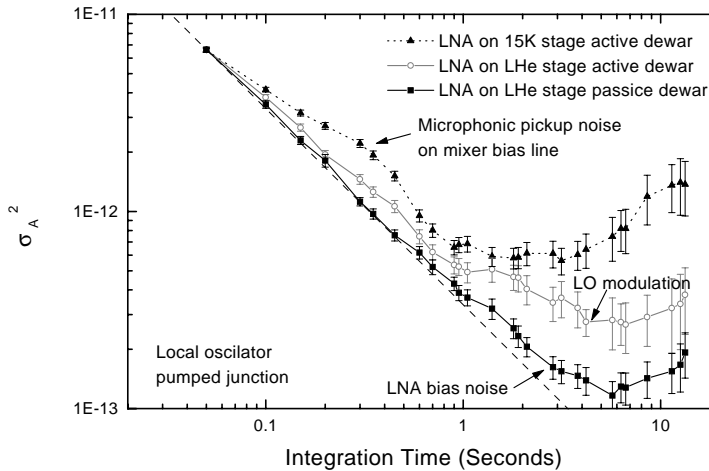


Fig. 10. LO Pumped cross slot with Josephson currents nulled out. The IF low noise amplifier was mounted in a IR-Lab liquid helium dewar, and CTI cooled hybrid dewar. In the hybrid dewar the LNA was mounted in two ways; directly to the 15K actively cooled stage and to the LHe stage. In the passive dewar Josephson instability, or SIS bias noise induced gain instability, shows up at 6 seconds! In the active hybrid dewar acoustic LO modulation becomes apparent for integration times between 1 and 6 seconds.

degraded from 6 seconds to ≈ 4 seconds, but the “Allan” variance also begins to significantly deviate from the ideal $\frac{1}{7}$ slope at approximately 1 second. The CTI compressor has a 1.2 Hz cycle, and it is hypothesized that the local oscillator and beamsplitter are modulated at a harmonic of the cryo-cooling cycle.

Finally, when we mount the LNA at the 15K stage, we observe a further decrease in “Allan” variance time to 1.5 seconds. In this experiment we observe the net effect of acoustic vibrations of the LNA, micro-phonic noise on the LNA and SIS-mixer bias lines, mechanical vibrations of the LO chain (including beamsplitter), and Josephson noise suppression in the junction. This combined effect is in very good agreement to what has been measured at the observatory (Fig. 9). Loss in integration efficiency is now observed to occur at just 0.1 seconds.

Fig. 11 shows the effect of Josephson oscillations on the mixer stability. With the magnetic field (used to suppress Josephson currents) switched off, the “Allan” variance stability time of the receiver was reduced to a mere 0.8 seconds. In all these experiments we have used a 100 MHz bandpass filter.

XI. IMPLICATIONS TO RADIO ASTRONOMY

The results presented suggest that the mechanical perturbation of cryo-coolers can cause astronomical observations of narrow linewidth galactic sources to deviate from theory when integration’s exceed ~ 10 seconds (given a spectrometer frequency resolution of 1 MHz).

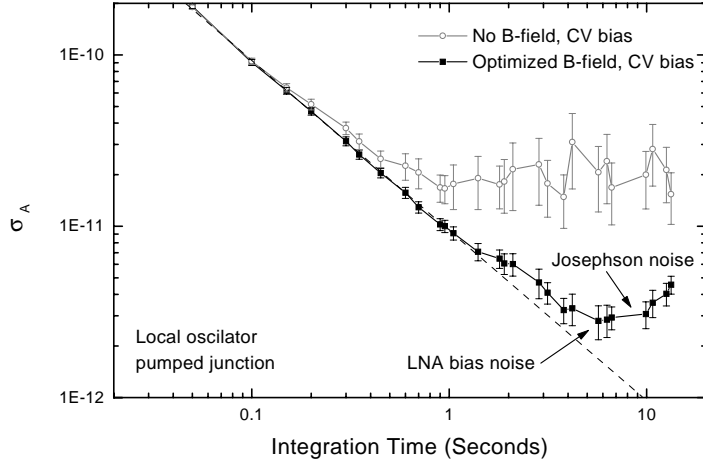


Fig. 11. LO Pumped Dual polarization cross slot with and without applied magnetic field. Data taken in a passive cooled dewar.

Indeed, such behavior is often observed. In the past, the dominant source of such deviations has been believed to be variations in atmospheric opacity, referred to as sky-noise. Our results suggest that in some instances, especially under good sky conditions, the instrument itself may produce the limiting instabilities. The popular use of closed cycle LHe coolers is likely to aggravate the situation with the introduction of small scale periodic temperature fluctuations in the mixer (Fig 7), this in addition to the acoustical noise effects discussed earlier.

On single aperture telescopes, the best way to avoid instability induced observing inefficiencies is to use a chopping secondary. This ‘beam switching’ technique allows the observer to switch between ‘on’ and ‘off’ source positions at frequencies up to several Hertz, thus largely eliminating the $1/f$ noise instabilities of the receiver system.

Note that such ‘beam-switched’ observations can only be used when the astronomical source emission region is no more than a few telescope beamwidths in extent. For more extended sources, an on-off position switching strategy is often employed. However, if the observers are limited to integration times of 10 seconds or less, they may find themselves spending more time slewing the telescope between positions than actually taking data. On the other hand, if integrations longer than 10 seconds are allowed, baseline subtraction suffers and integration efficiency is expected to be poor. An alternative observing mode is ‘on-the-fly’ (OTF) mapping. Here the telescope is allowed to scan through the source while averaging the data in short (typically ~ 3 sec) bins. When atmospheric conditions are good (≤ 1 mm of precipitable water vapor) ‘on’ scans can last for upwards of 120 seconds before a single ‘off’ scan is taken, thereby minimizing the loss in time associated with slewing the telescope between ‘on’ and ‘off’ positions. However, even when the ‘OTF’ mapping technique is used observing efficiency and proper baseline subtraction will improve if the receiver stability is

increased.

When SIS receivers are used for large continuum or low resolution extragalactic observations only fast ‘beam switching’ operation seems appropriate.

Finally, it should be noted that interferometers (multiple telescope’s used together to synthesize a single large diameter telescope) are by their nature much more tolerant of gain fluctuations than single dish receivers. This because only correlated signals will appear at the output of the spectrometer while uncorrelated signals such as receiver instabilities will not. Note however that this does not negate the importance of high integration efficiency, and hence having receivers with suitable long stability (“Allan” variance) times.

XII. CONCLUSION

A detailed study on the output noise stability of SIS receivers is presented. We have investigated the destabilizing effects of acoustic vibrations on a low noise amplifier (LNA) and local oscillator (LO) chain, micro-phonic noise on the LNA and SIS mixer bias lines, SIS constant voltage feedback bias noise, Josephson oscillation noise, and finally thermal drift noise of the SIS mixer and low noise amplifier.

In the process we found that fundamentally the SIS mixer is stable to at least 6 seconds in a 100 MHz bandwidth. This limit is set by how well one is able to suppress the Josephson effect in the superconducting tunnel junction and possibly also by SIS mixer bias noise, which modulates the mixer gain. In practice though the Josephson effect does not limit the stability of SIS receivers, rather the stability of the receiver is set by numerous external factors.

In a passive cooled dewar we have measured “Allan” variance stability times up to 9 seconds with an above the energy gap biased SIS mixer (IF bandwidth = 100 MHz). The “Allan” variance time in this case is limited by the room temperature IF total power amplifier and measurement setup.

In an active cooled hybrid style dewar the situation was much worse. With the low noise amplifier mounted on the 15K active cooled stage we measure an “Allan” variance time of 1.5 seconds, both at the observatory and in the laboratory. Vibration isolating the low noise amplifier gives a significant stability improvement, however the exact amount of improvement is very much dependent on the amplifier design and employed mounting scheme.

In the lab we did not observe a difference in the “Allan” variance stability time of the receiver when the junction was biased in closed feedback, or open loop mode. At the observatory, due to the large EMI/RFI noise environment, we did in fact notice a significant change.

The mixer gain of a Local Oscillator pumped SIS junction has been measured and is observed to be a strong and negative function of temperature. The mixer’s peak sensitivity to temperature change appears to be at approximately 4.9 Kelvin. The low noise amplifier (GaAs HEMT’s) in contrast has a small, linearly varying, and positive temperature dependence. Cooling the mixer below 3K improves the mixer gain by 10%, but even more importantly reduces the mixer’s susceptibility to LHe bath temperature fluctuations. In high resolution spectrometer mode with a channel bandwidth of 100 KHz, 1 second of “Allan” stability time and an high altitude Helium bath temperature of 3.6 Kelvin, we find a maximum allowed temperature fluctuation of 106 mK/second for the LNA and 48 mK/second for the

SIS mixer. At 4.2 Kelvin the allowed SIS mixer temperature fluctuation has been reduced to 13.8 mK/second. These numbers are upper limits, and for wide bandwidth continuum or course resolution extragalactic observations the result is much more stringent.

Finally, high mobility transistor (HEMT) gain fluctuations, if any, appear to be at least an order of magnitude below such noise sources as acoustic vibrations, bias line noise due to high EMI/RFI noise environment, and problems with Josephson noise suppression.

It is recommended that special attention be given to minimize microphonic pickup in the LNA and Local Oscillator chain. Temperature fluctuations should be kept at a minimum, especially so when the mixer is operated at a Helium bath temperature of 4.2 Kelvin. In a high noise environment such as an observatory, it may be advisable to use several different feedback loop time constants, depending on the mode of operation. And finally a resistive divider network in the SIS and LNA bias line should at all cost be implemented.

XIII. ACKNOWLEDGMENTS

We wish to thank Jonas Zmuidzinas and Frank Rice of Caltech for very helpful discussions on the fundamental physics of SIS mixers, Chris Walker of the University of Arizona, Dave Woody of Caltech, and John Carlstrom of the University of Chicago for their input regarding the implications of receiver instability to Radio Astronomy, and Sander Weinreb of JPL for his thoughts on LNA gain stability. This work was supported in part by NSF grant# AST-9615025.

REFERENCES

- [1] J.D. Kraus, "Radio Astronomy", *2nd Edition*, pp7-8
- [2] D. W. Allan, "Statistics of Atomic Frequency Standards", *Proc. IEEE*, Vol. 54, No. 2, pp 221-230, 1969
- [3] A.B Barnes, "Characterization of frequency stability", *IEEE Trans. Instrument Measurements*, Vol. IM-20, No. 2, pp 105-120, 1971
- [4] R. Schieder, "Characterization and Measurement of System Stability", *SPIE, Vol 598*, Instrumentation for Submillimeter Spectroscopy (1985)
- [5] B.D. Josephson, "Possible new effects in superconductive tunneling", *Phys. Letters 1*, (1962) pp 251-253
- [6] R. Bradley, *NRAO*, Private Communication
- [7] S. Padin, "A Cooled 1-2 GHz balanced HEMT amplifier", *IEEE, Microwave Theory and Techniques*, Vol 39, No. 7, pp. 1239-1243 (1991)
- [8] *Infrared Laboratories, Inc.* 1808 East 17th Street, Tuscon, Az 85719
- [9] B.N Ellison, "A low noise 230 GHz SIS receiver", *Int. J. Infrared and Millimeter waves*, Vol. 8, pp. 609-625, June 1987
- [10] CTI-Cryogenics, Helix Technology Corporation, Nine Hampshire Street, Mansfield, MA 02048, USA.
- [11] Personal communication
- [12] G. Chattopadhyay, D. Miller, H. G. LeDuc, and J. Zmuidzinas, "A 550-GHz Dual Polarized Quasi-Optical SIS Mixer," *Proceedings of the Tenth International Symposium of Space Terahertz Technology*, Charlottesville, Virginia, pp. 130-143, March 16-18, 1999.
- [13] J. W. Kooi , M. Chan, B. Bumble, and T. G. Phillips, "A low noise 345 GHz waveguide receiver employing a tuned $0.50 \mu\text{m}^2$ Nb/AlO_x/Nb tunnel junction," *Int. J. IR and MM Waves*, vol. 15, No. 5, May 1994.
- [14] J.W. Kooi, J. Pety, B. Bumble, C.K. Walker, H.G. LeDuc P.L. Schaffer, and T.G. Phillips, "A 850 GHz Waveguide Receiver employing a Niobium SIS Junction Fabricated on a 1um Si3N4 Membrane," *IEEE Transactions on Microwave Theory and Techniques*, Vol. 46, No. 2, pp151-161, February 1998.